BJCP British Journal of Clinical Pharmacology

DOI:10.1111/j.1365-2125.2011.03963.x

Population pharmacokinetic analysis of sorafenib in patients with solid tumours

Lokesh Jain,[1,6] Sukyung Woo,[1] Erin R. Gardner,[3] William L. Dahut,[2] Elise C. Kohn,[2] Shivaani Kummar,[2] Diane R. Mould,[4] Giuseppe Giaccone,[2] Robert Yarchoan,[5] Jürgen Venitz[6] & William D. Figg[1,2,6]

[1]Clinical Pharmacology Program, [2]Medical Oncology Branch, National Cancer Institute, NIH, Bethesda, MD 20892, [3]Clinical Pharmacology Program, SAIC-Frederick, Inc., NCI-Frederick, Frederick, MD 21702, [4]Projections Research, Inc., Phoenixville, PA 19460, [5]HIV and AIDS Malignancy Branch, National Cancer Institute, NIH, Bethesda, MD 20892 and [6]Department of Pharmaceutics, School of Pharmacy, Virginia Commonwealth University, Richmond, VA 23298, USA

Correspondence
Dr William D. Figg Pharm D, Medical Oncology Branch, CCR, NCI/NIH, 9000 Rockville Pike, Building 10, Room 5A01, Bethesda, Maryland 20892, USA.
Tel.: +1 301 402 3622
Fax: +1 301 402 8606
E-mail: wdfigg@helix.nih.gov

Keywords
CYP3A4, population pharmacokinetics, sorafenib, tyrosine kinase inhibitor, UGT1A9

Received
10 July 2010
Accepted
6 March 2011
Accepted Article
11 March 2011

WHAT IS ALREADY KNOWN ABOUT THIS SUBJECT

- Sorafenib is a multikinase inhibitor with activity against B-raf, C-raf, VEGFR2, PDGFRβ and FGFR1.
- Sorafenib is clinically approved for the treatment of renal cell carcinoma (RCC) and hepatocellular carcinoma (HCC).
- The pharmacokinetics (PK) of sorafenib are highly variable between subjects.
- Sorafenib exposure increases less than dose proportionally (likely due to limited solubility).
- Sorafenib undergoes enterohepatic recycling (EHC).

WHAT THIS STUDY ADDS

- This is the first study to characterize the PK of sorafenib using a model based on sorafenib's known disposition characteristics such as delayed/solubility-limited GI absorption and EHC. The parameterization of the EHC model used a square wave function to describe the gall bladder emptying.
- This study evaluated the effect of baseline bodyweight, BSA, age, gender, liver function parameters, kidney function parameters and genotype with respect to CYP3A4*1B, CYP3A5*3C, UGT1A9*3 and UGT1A9*5 on sorafenib PK. No clinically important covariates were identified.
- This model can be used to simulate and explore alternative dosing regimens and to develop exposure–response relationships for sorafenib.

AIMS

To characterize the pharmacokinetics (PK) of sorafenib in patients with solid tumours and to evaluate the possible effects of demographic, clinical and pharmacogenetic (CYP3A4*1B, CYP3A5*3C, UGT1A9*3 and UGT1A9*5) covariates on the disposition of sorafenib.

METHODS

PK were assessed in 111 patients enrolled in five phase I and II clinical trials, where sorafenib 200 or 400 mg was administered twice daily as a single agent or in combination therapy. All patients were genotyped for polymorphisms in metabolic enzymes for sorafenib. Population PK analysis was performed by using nonlinear mixed effects modelling (NONMEM). The final model was validated using visual predictive checks and nonparametric bootstrap analysis.

RESULTS

A one compartment model with four transit absorption compartments and enterohepatic circulation (EHC) adequately described sorafenib disposition. Baseline bodyweight was a statistically significant covariate for distributional volume, accounting for 4% of inter-individual variability (IIV). PK model parameter estimates (range) for an 80 kg patient were clearance 8.13 l h^{-1} (3.6–22.3 l h^{-1}), volume 213 l (50–1000 l), mean absorption transit time 1.98 h (0.5–13 h), fraction undergoing EHC 50% and average time to gall bladder emptying 6.13 h.

CONCLUSIONS

Overall, population PK analysis was consistent with known biopharmaceutical/PK characteristics of oral sorafenib. No clinically important PK covariates were identified.

Introduction

Sorafenib, a multikinase inhibitor, is approved for the treatment of advanced renal cell carcinoma and/or hepatocellular carcinoma in more than 80 countries [1]. Sorafenib is a potent inhibitor of wild-type B-raf, oncogenic *B-raf*V6600E, C-raf and pro-angiogenic receptor tyrosine kinases (namely VEGFR1, 2, 3, PDGFRβ and FGFR1) [2]. Sorafenib inhibited tumour growth and angiogenesis of human hepatocellular carcinoma and renal cell carcinoma, and several other human tumour xenografts in immunocompromised mice [3]. In a colon cancer (HCT cell line) xenograft model, after 14 days of once daily treatment sorafenib reduced the tumour size by 45% at 10 mg kg^{-1}, 64% at 30 mg kg^{-1}, 68% at 100 mg kg^{-1} and 33% at 300 mg kg^{-1} doses [2].

Clinical studies involving sorafenib reported a high degree of inter-individual variability (IIV) in pharmacokinetics (PK), clinical efficacy and adverse event profiles. The magnitude of variability (%CV) on sorafenib exposure (area under the plasma concentration–time curve, AUC) ranged from 5–83% and that for peak plasma concentrations (C_{max}) from 33–88% at oral doses of 200 or 400 mg given twice daily [4–7]. The median time to peak plasma concentration (t_{max}) varied from 2–9.5 h [4–7]. Plasma concentrations of sorafenib achieved steady-state after approximately 7 days of multiple dose administration, without any further drug accumulation thereafter [4]. In single dose escalation studies, a less than proportional increase in AUC and C_{max} was observed with increasing doses of sorafenib, reaching a plateau at 600 mg twice daily [8], likely as a result of limited gastrointestinal (GI) solubility of sorafenib. The aqueous solubility for the sorafenib tosylate salt ranges from 0.034 mg 100 ml^{-1} at pH 1.0 to 0.013 mg 100 ml^{-1} at pH 4.5 [9], which approximates to <1 mg 250 ml^{-1} water, suggesting that clinical doses are likely exceeding the GI solubility. In *in vitro* cellular and preclinical studies, sorafenib was found to be highly permeable across GI epithelia [9], possibly classifying sorafenib as a class II or IV drug in the biop harmaceutics classification system (BCS) [10]. Sorafenib is also thought to be subject to enterohepatic circulation (EHC), based on its biliary xcretion in bile duct cannulated rats [9] and the occurrence of typical double peaks in the plasma concentration–time profiles from patients treated with sorafenib [9].

Sorafenib is known to be primarily metabolized by hepatic CYP3A4 and UGT1A9 enzymes [3]. Genetics are believed to account for 70–90% of the variation in expression and metabolic activity of CYP3A isoenzymes [11]. CYP3A4*1B and CYP3A5*3C, the most commonly studied variants of *CYP3A4* and *CYP3A5*, have a respective variant allele frequency of 3.6–9.6% and 90% in Caucasians and 53–67% and 50% in African-Americans [12]. The CYP3A4*1B is a promoter site polymorphism and CYP3A5*3C has shown to result in production of truncated protein, both of which may decrease the expression or activity of these metabolic isoenzymes and may potentially affect the PK of sorafenib [12, 13]. A recent report demonstrated ~3-fold increase in sorafenib steady-state concentrations following co-administration with felodipine, indicating the possibility of CYP3A4 based drug–drug interactions [14]. Only a few studies have investigated the impact of *UGT1A9* polymorphisms on drug disposition. UGT1A9*3 and UGT1A9*5 SNPs are located in the coding region and result in complete or partial inactivation of glucuronidation activity for prototypical substrates such as SN-38 [15]. Co-administration of sorafenib with irinotecan 125 mg m^{-2}, increased mean sorafenib AUC(0,10 h) and C_{max} by 68% and 78%, respectively [16]. This indicates the possibility of UGT enzyme based drug–drug interaction [3]. The frequency of the UGT1A9*3 heterozygous genotype (*1/*3) in Caucasians is 4.4% [17] and only one study examined UGT1A9*5 polymorphism in Caucasians and found no variant carriers [18].

The objectives of this study were (a) to describe the PK of sorafenib by a population pharmacokinetic (PPK) approach and (b) to identify the covariates possibly contributing to the variability in PK. The patients were enrolled in phase I and II clinical trials at the National Cancer Institute (NCI), which evaluated safety and/or activity of sorafenib in patients with metastatic castrate-resistant prostate cancer (mCRPC), non-small cell lung cancer (NSCLC), colorectal cancer (CRC), Kaposi's sarcoma (KS) and other solid tumours. In this report, we describe the findings of the PPK analysis, including the individual and mean PPK model parameters, their associated IIVs and covariates possibly contributing to PK variability.

Methods

Patients, data collection and genotyping analysis

A summary of phase I/II studies involved in the current analysis is presented in Table 1. Sorafenib was administered at doses of 200 or 400 mg twice daily as a single agent or in combination with other therapies. All of the studies were single arm, single centre, open label trials and were conducted at the NCI. The clinical protocols were approved by the Institutional Review Board and informed consent was obtained from every patient prior to enrolment. Enrolment was restricted to patients with normal organ function and age ≥18 years. Patients with mCRPC and NSCLC received the approved dose of sorafenib (400 mg twice daily) as a single agent, and patients with CRC were treated with sorafenib 400 mg twice daily in combination with cetuximab (400 mg m^{-2} i.v. loading dose in week 1, followed by 250 mg m^{-2} i.v. weekly). Patients with other solid tumours received sorafenib 200 mg twice daily with or without bevacizumab 5 mg kg^{-1} i.v. biweekly. Patients with Kaposi's sarcoma were enrolled into a dose escalation trial in which they received sorafenib as either a

Table 1

Description of clinical trials and patients included in the analysis

Trial type	Tumor type	Number of patients	Treatment/dosage	Number of patients for PK sampling	
				Initial dose	Steady-state
Phase II	Metastatic castrate resistant prostate cancer	46	Sorafenib 400 mg twice daily in continuous cycles	46	–
Phase II	Non-small cell lung cancer	18	Sorafenib 400 mg twice daily in continuous cycles	18	17
Phase II	Colorectal cancer	18	Sorafenib 400 mg twice daily in continuous cycles + cetuximab 400 mg m^{-2} loading dose in week 1, followed by 250 mg m^{-2} i.v. weekly	18	–
Phase I	Solid tumours	28	Sorafenib 200 mg twice daily in continuous cycles ± bevacizumab 5 mg kg^{-1} i.v. biweekly	28	12
Phase I	Kaposi's sarcoma	2	Sorafenib 200 mg twice daily in continuous cycles	–	2

single agent (at a starting dose of 200 mg twice daily) or in combination with a protease inhibitor (starting dose for sorafenib 200 mg once daily). Data from patients with Kaposi's sarcoma receiving only sorafenib were included in this analysis because of the potential for a drug interaction. All enrolled patients were genotyped for CYP3A4*1B, CYP3A5*3, UGT1A9*3 and UGT1A9*5 single nucleotide polymorphisms (SNPs) using methods described elsewhere [18, 19]. Deviation from Hardy-Weinberg equilibrium (HWE) was assessed by Chi-square statistics. HWE provides a means to compare the actual genetic distribution of the population under consideration with the genetic distribution we would expect if the population was not evolving (i.e. remains in HWE).

Pharmacokinetic sampling and sample analysis

Serial blood samples were drawn up to 12 h post first dose at 0, 0.25, 0.5, 1, 2, 4, 6, 8 and 12 h, with one additional sample collected 12 h after the subsequent, second dose. Samples were also drawn at steady-state at the same time points for selected patients (Table 1). These samples were analyzed for sorafenib by using a validated liquid chromatographic method with mass spectrometric detection [20]. The calibration curve range was 5–2000 ng ml^{-1}. The accuracy and precision of this method ranged from 92.9–99.9% and 95.5–98.3%, respectively [20]. Concentrations below the lower limits of quantification (LLOQ) of 5 ng ml^{-1} were included in the analysis as long as they appeared to be above the lower limit of detection (LLOD) of 0.2 ng ml^{-1} for the bioanalytical method, with chromatogram shape clearly distinguishable from blank samples. Quality control (QC) samples were tested at low, medium and high concentrations of 8 ng ml^{-1}, 160 ng ml^{-1} and 1600 ng ml^{-1}, respectively. The interday and intraday %CV for low, medium and high QC concentrations were 4.6% and 4.2%, 4.4% and 2.4%, and 6.2% and 1.1%, respectively. The %CV acceptance criterion for all QC samples tested during analysis of patient samples was less than ± 15%.

Pharmacokinetic analysis

The PPK model development and simulations were performed by non-linear mixed effect modelling using NONMEM version VI level 2.0 (ICON Development Solutions, Ellicott City, MD). NONMEM was compiled by Intel Visual Fortran compiler version 10 (Intel Corporation, Santa Clara, CA) on a Windows XP operating system. Unless otherwise stated, all estimations were carried out using the first order conditional estimation method with the interaction option (FOCEI). Data processing and statistical analyses were performed using JMP statistical software version 8.0 (SAS Institute, South Cary, NC). Graphical diagnostics were assessed using Xpose version 4 (Uppsala University, Sweden) and S-PLUS (7.0, Insightful, Palo Alto, CA).

Selection of structural PK model

One and two compartment models with components to describe the delayed and variable absorption of sorafenib and EHC were tested as initial structural models. Several absorption models, including first or zero order absorption models with lag time, parallel and sequential mixed zero and first order absorption (with or without lag time), and parallel and sequential GI transit absorption compartments, were evaluated [21]. EHC was modelled using various forms of caternary compartment(s) between the central (systemic circulation) and absorption compartment(s) to mimic the physiologic recycling as a regular or controlled process, regulated by periodic functions or dummy compartments [21–24]. Meal times were not recorded in the data set and hence were not used as an index of gall bladder emptying. Time after dose was used as a marker of gall bladder emptying, assuming that all patients received the same dosing schedule.

A log transformation of both sides (LTBS) approach was used, where the logarithms of observed plasma concentrations were fitted by the PK model to predict the log transformed concentrations. An exponential model was used to describe the IIV in PK parameters. Covariance and interoccasion variability (IOV) in PK parameters were also evaluated. A combined proportional and additive error model

was used to describe the residual random error in plasma concentrations as described in equation 1 [25].

$$Ln(C_{ij}) = Ln(\hat{C}_{ij}) + \sqrt{\varepsilon_{ij_1}^2 + \frac{\varepsilon_{ij_2}^2}{\hat{C}_{ij}^2}} \quad (1)$$

where C_{ij} is the j^{th} plasma concentration measured in the i^{th} individual, $\hat{C}_{ij}$ is the individual model-predicted plasma concentration, and ε_{ij1} and ε_{ij2} are the proportional and additive components, respectively.

Covariate models

The candidate covariates screened during PPK model building included 'trial', 'dose' and parameters listed in Table 2. Creatinine clearance and body surface area (BSA) were calculated using Cockcroft-Gault and Dubois & Dubois formulae, respectively. There were no missing values for covariates, except the genotype data for few patients whose DNA could not be amplified. For missing covariates, fixed effects were estimated separately during covariate model building. Graphical and statistical relationships between *post hoc* Bayesian estimates of η and covariate values were used to identify candidate covariates, where η represents the random difference between typical population mean values of model parameters and individual specific model parameters. Covariate model building was accomplished by mixed stepwise forward addition ($P < 0.05$) and stepwise backward elimination ($P < 0.001$), based on change in OFV, as well as reductions in IIV and model completion status (e.g. successful convergence or termination). Covariates were included in their respective PK model parameters as allometric/linear models. Multiplicative equations were used to describe the combined effect of multiple covariates on the same parameter.

Goodness-of-fit plots examined for each model included: (a) scatter plots of observed (DV), population and individual predicted (PRED and IPRED) concentrations *vs.* time, (b) observed *vs.* predicted concentrations (DV *vs.* PRED or DV *vs.* IPRED) and (c) weighted residuals *vs.* time or IPRED. In addition, η-shrinkage [26] and quantile-quantile (QQ) plots for η were assessed for all parameters. IIV for

Table 2

Patient characteristics at screening for each clinical trial and for total patients ($n = 111$)

Parameter	PC ($n = 46$)	NSCLC ($n = 18$)	CRC ($n = 18$)	ST ($n = 28$)	KS ($n = 2$)	Total
Demographics	Median (range) or N (%)					
Age (years)	65.1 (48.6–84.9)	67.5 (35.0–84.7)	56.7 (37.1–75.4)	58.8 (30.3–76.0)	(60.9–66.6)	63.9 (30.3–84.9)
Bodyweight (kg)	93.8 (50.1–131.3)	66.7 (35.2–93.2)	81.9 (40.6–107.2)	74.2 (50.9–120.3)	(92.3–94.0)	81.4 (35.2–132.5)
BSA (kg m^{-2})	2.1 (1.5–2.5)	1.7 (1.2–2.1)	1.7 (1.3–2.3)	1.9 (1.5–2.5)	(2.0–2.2)	1.9 (1.2–2.5)
Gender, male/female	46 (100)/	11 (61)/	9 (50)/	10 (36)/	2 (100)/	77 (69)/
	0 (0)	7 (39)	9 (50)	18 (64)	0 (0)	34 (31)
Ethnicity, Caucasian/	38 (82)/	12 (66.7)/	13 (72.2)/	27 (96)/	1 (50)/	90 (81)/
AA/	5 (11)/	2 (11.1)/	3 (16.7)/	0 (0)/	1 (50)/	12 (11)/
others	3(7)	4 (22.2)	2 (11.1)	1 (4)	0 (0)	9 (8)
Clinical	Median (range)					
Albumin (g l^{-1})	37 (22–44)	34 (28–43)	36 (28–41)	36 (31–42)	(38–41)	36 (22–44)
Total protein (g l^{-1})	65 (46–80)	67 (60–79)	68 (53–73)	67 (54–74)	(67–76)	66 (46–80)
Alkaline phosphatase (U l^{-1})	80 (35–414)	74 (51–126)	84 (54–249)	89 (34–199)	(60–87)	82 (34–414)
Total bilirubin (μmol l^{-1})	10.3 (1.7–20.5)	10.3 (6.8–18.8)	12.0 (3.4–20.5)	10.3 (3.4–29.1)	(13.7–23.9)	10.3 (1.7–29.1)
AST (U l^{-1})	28 (13–90)	22 (13–42)	29 (19–45)	27 (15–47)	(22–38)	26 (13–90)
ALT (U l^{-1})	21 (8–75)	18 (9–43)	21 (13–34)	24 (9–63)	(18–39)	21 (8–75)
S_{Cr} μmol l^{-1}	79.6 (53.0–132.6)	88.4 (53.0–132.6)	70.7 (35.4–114.9)	79.6 (53.0–168)	(88.4–106.1)	79.6 (35.4–168)
CL_{Cr} (ml s^{-1})	1.70 (0.43–3.33)	1.26 (0.57–2.27)	1.67 (0.78–3.10)	1.60 (0.87–3.77)	(1.41–1.60)	1.59 (0.43–3.77)
Genetic	(wt/het/var) *n* (%)					
CYP3A4*1B	37 (80.1)/	17 (94.4)/	11 (68.8)/	25 (92.6)/	0 (0)/	89 (82.4)/
	5 (10.9)/	0 (0)/	2 (12.5)/	2 (7.4)/	1 (50)/	10 (9.3)/
	4 (8.7)	1 (5.6)	3 (18.7)	0 (0)	1 (50)	9 (8.3)
CYP3A5*3C	7 (8.7)/	1 (5.9)/	1 (5.9)/	1 (3.7)/	1 (50)/	8 (7.4)/
	4 (8.7)/	4 (23.5)/	3 (17.6)/	6 (22.2)/	0 (0)/	17 (15.7)/
	38 (82.6)	12 (70.6)	13 (76.5)	20 (74.1)	1 (50)	83 (76.9)
UGT1A9*3	43 (95.6)/	17 (100)/	16 (94.1)/	26 (96.3)/	2 (100)/	103 (96.3)/
	1 (2.2)/	0 (0)/	1 (5.9)/	1 (3.7)/	0 (0)/	3 (2.8)/
	1 (2.2)	0 (0)	0 (0)	0 (0)	0 (0)	1 (0.9)
UGT1A9*5	45 (100)/	18 (100)/	17 (100)/	26 (100)/	2 (100)/	107 (100)/
	0 (0)/	0 (0)/	0 (0)/	0 (0)/	0 (0)/	0 (0)/
	0 (0)	0 (0)	0 (0)	0 (0)	0 (0)	0 (0)

AA, African American; ALT, alanine aminotransferase; AST, aspartate aminotransferase; BSA, body surface area; CL_{Cr}, estimated creatinine clearance; CRC, colorectal cancer; het, heterozygous genotype; KS, Kaposi's sarcoma; NSCLC, non-small cell lung cancer; PC, prostate cancer; S_{Cr}, serum creatinine; ST, solid tumour; var, homozygous variant genotype; wt, wild type genotype.

parameters with high η-shrinkage were not estimated. The QQ plots assess the underlying assumption of normal distribution for η random effects.

Final PPK model evaluation

The stability and predictive performance of models were assessed by an unstratified nonparametric bootstrap analysis, assessment of the relative error (RE) and the root mean square error (RMSE), and visual predictive checks (VPC). For the non-parametric unstratified bootstrap analysis 2284 bootstrap replicates were generated and the results from all replicates were used to calculate the median and the 95% confidence interval for the PPK model parameters. In addition the percentage of successful convergence for the bootstrap replicates was also monitored. RE and RMSE were calculated using the equations 2 and 3. RE and RMSE were summarized by descriptive statistics.

$$RE_{ij}(\%) = \frac{Ln(\hat{C}_{ij}) - Ln(C_{ij})}{Ln(C_{ij})} \cdot 100 \quad (2)$$

$$RMSE = \frac{\sum_{i=1}^{m} \sqrt{\frac{\sum_{j=1}^{n} (\hat{C}_{ij} - C_{ij})^2}{n}}}{m} \quad (3)$$

where C_{ij} and $\hat{C}_{ij}$ were the same as described above for equation 1. n and m represent the total number of observations for an individual subject and total number of subjects, respectively.

For the VPC, the final model and parameter estimates were used to simulate the data for 10 000 virtual patients. Simulated plasma concentration–time profiles were dose-normalized, which were then binned on nominal time points and the 5th, 25th, 50th (median), 75th and 95th percentiles were calculated. Distribution of simulated concentrations was then visually compared with the measured sorafenib concentrations and their median at each sampling time point.

Results

Data

Typical sorafenib plasma concentrations *vs.* time profiles from selected patients are shown in Figure 1A. After oral administration of sorafenib, absorption was slow and delayed with t_{max} values ranging from 2–12 h. Approximately 8% of patients had distinct secondary peaks in their profiles, characteristic for EHC. For other patients, although distinct double peaks were not observed, the terminal phase was rather flat, suggesting the presence of EHC. Of the 112 patients with variable concentration data, one was excluded from PPK analysis because of extremely low plasma concentrations compared with others (on average approximately 30-fold lower with approximately a 9-fold difference in C_{max}), which could destabilize the model. The studied demographics, liver and kidney function test values and genotype for metabolic enzymes for this patient were comparable with other patients and there was no apparent reason for these low concentrations. Overall, a total of 1249 sorafenib concentrations were used for PPK model building, of which 3.3% were below the LLOQ and were reported as actual values. For Caucasian patients, which represented approximately 80% of the patient population, the CYP3A4*1B and CYP3A5*3 genotype frequencies were in HWE. The UGT1A9*3 polymorphism did not follow HWE, which is likely due to the small number of patients found carrying the UGT1A9*3 variant. None of the patients carried the variants for UGT1A9*5 polymorphisms and hence, HWE was not assessed.

Pharmacokinetics

The final PPK model was a one compartment model with additional components describing the observed absorption delay and underlying EHC, as shown in Figure 1B and described by equations 4 to 10. The initial delay in quantifiable plasma concentrations was adequately described by the GI transit compartments absorption model. Four transit compartments, each of them receiving drug from the antecedent and releasing drug into the subsequent transit compartment with a first order rate constant k_a, accommodated the apparent lag time and a highly variable t_{max}. EHC was modelled with a semi-mechanistic model, where a fraction of drug from the central compartment (F_{ent}) was hepatobiliary excreted (transferred) into a gall bladder compartment with a first order rate k_b, which, in turn, periodically emptied drug into the last GI transit compartment at a first order rate of k_{Ehc}. For modelling purposes, F_{ent} was logit transformed, to constrain its value between 0 and 1, and to allow typical parameters to be estimated as a continuous function (–infinity to +infinity). The periodic drug release from the gall bladder compartment was regulated by the on-off switch '*Ehc*', using a sigmoidal function with a large Hill coefficient, such that '*Ehc*' mimics a square wave function analogous to gall bladder emptying (Figure 2). A large Hill coefficient increased the steepness of the '*Ehc*' function to mimic an all or none response, without the numerical differentiation problems associated with use of discontinuous functions such as step functions or lag times. t' was the time of emptying. At times less than t', the value of EHC was 0 and the gall bladder did not empty and at times greater than t' the value of EHC was 1 and the gall bladder emptied. The remaining fraction in the central compartment ($1 - F_{ent}$), was eliminated with a first order rate constant of k_e, reflecting hepatic metabolism and any irreversible loss including the biliary loss which was not recirculated; k_e was parameterized in terms of apparent clearance (CL/*F*) and volume of distribution (*V*/*F*).

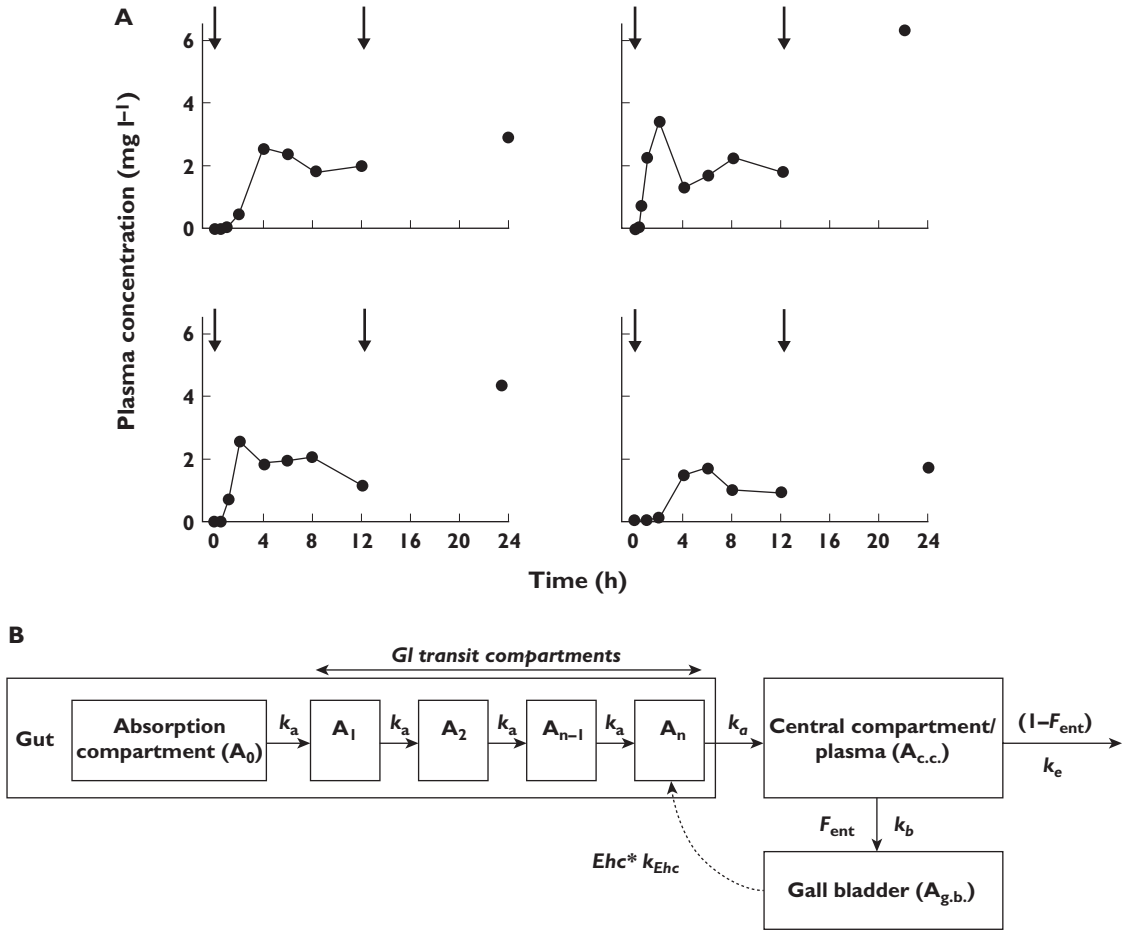

Figure 1

(A) Typical plasma concentration–time profiles from four different patients receiving 400 or 200 mg of sorafenib twice daily. (B) Schematic representation of the final PPK model. Arrow(↓): time of dose administration, k_a first order absorption rate constant, k_e(= CL/*V*) first order elimination rate constant, k_b first-order rate constant for excretion of drug from central compartment to gall bladder, k_{Ehc} first order rate constant for recirculation of drug from gall bladder to absorption compartments, F_{ent} fraction of dose undergoing enterohepatic recirculation, *Ehc* square-wave function, A_0 amount in absorption compartment, A_n amount in nth transit compartment, $A_{c.c.}$amount in central compartment, $A_{g.b}$ amount in gall bladder

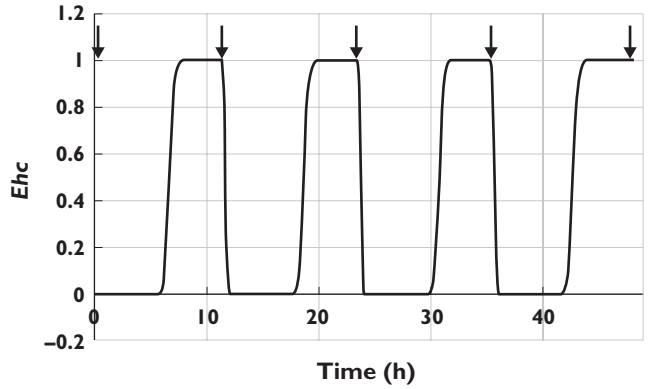

Figure 2

Change in *Ehc* across time after a single dose of sorafenib based on equation 10 for $t' = 6.7$ h. Arrows indicate time of dose administration

$$\frac{dA_0}{dt} = -k_a \cdot A_0 \quad (4)$$

$$\frac{dA_1}{dt} = -k_a \cdot (A_1 - A_0) \quad (5)$$

$$\vdots$$

$$\frac{dA_3}{dt} = -k_a \cdot (A_3 - A_2) \quad (6)$$

$$\frac{dA_4}{dt} = -k_a \cdot (A_4 - A_3) + Ehc \cdot k_{Ehc} \cdot A_{g.b.} \quad (7)$$

$$\frac{dA_{c.c.}}{dt} = k_a \cdot A_4 - F_{ent} \cdot k_b \cdot A_{c.c.} - (1 - F_{ent}) \cdot \frac{CL}{V} \cdot A_{c.c.} \quad (8)$$

$$\frac{dA_{g.b.}}{dt} = F_{ent} \cdot k_b \cdot A_{c.c.} - Ehc \cdot k_{Ehc} \cdot A_{g.b.} \quad (9)$$

$$Ehc = \frac{(t-DT)^{40}}{(t-DT)^{40} + (t')^{40}} \quad (10)$$

where A_0, $A_{c.c}$ and $A_{g.b}$ are amounts of drug in absorption, central and gall bladder compartment, and their initial conditions were set to zero except A_0, which was assumed to contain the entire dose at time zero. DT is the dosing time.

We attempted to estimate separately k_b and k_e, and in addition also tested the assumption that $k_b = k_{ehc}$, but were not successful. The model assuming $k_b = k_e$ was stable and adequately described the EHC for sorafenib. IIV was estimated for CL/*F*, *V*/*F* and k_a. For all other parameters, ηs had either high shrinkage (i.e. >30%) or low precision; therefore, these ηs were fixed to zero. The covariance between CL/*F* and *V*/*F* was estimated, resulting in a reduction in objective function value (OFV) by 30 points. IOV, stratifying first dose and steady-state as separate occasions, was added only to CL/*F*, which reduced OFV by 44 points. Introduction of IOV for other parameters did not result in any significant change in OFV.

The majority of patients included in the current analysis were middle-aged Caucasian males, with nearly all laboratory values within their respective normal reference ranges (Table 2). The mean body weight for males was higher than that for females (87 kg *vs.* 71 kg, $P < 0.0001$). Baseline bodyweight was found to be a statistically significant covariate for *V*/*F* and was modelled as a power function with the exponent fixed to 1 [27]. Inclusion of bodyweight on *V*/*F* resulted in a drop in OFV by 16 points ($P < 0.001$), but was able to explain only 4% of IIV. Lean bodyweight was also evaluated and not found to be superior to normal bodyweight. The log normal variances on PK parameters for the models with and without bodyweight as covariate are shown in Table S1. The inclusion of body weight on volume of distribution reduces the log normal variances on both CL/*F* and *V*/*F* because both are correlated. Serum albumin and ALT were identified as being significant for *V*/*F* during the initial covariate evaluation, but were not retained in the final model because of statistically insignificant increases in OFV during stepwise backward elimination. Genetic polymorphisms in metabolic enzymes (i.e. CYP3A4*1B, CYP3A5*3C and UGT1A9*3) did not have a significant effect on any PK model parameter. No patient carried the variant allele for the UGT1A9*5 polymorphism (Table 2).

The final PPK model parameters based on available data from 111 patients are summarized in Table 3. Typical population parameters for a patient with a bodyweight of 80 kg were CL/*F* 8.13 l h^{-1} (IIV 18% and IOV 48%) and *V*/*F* 213 l (IIV 69%). The average time spent by sorafenib in travelling from the absorption compartments to the central compartment (i.e. mean absorption transit time, MAT), was estimated to be 1.98 h. The correlation coefficient between CL/*F* and *V*/*F* was 0.77. The estimates of shrinkage for IIV on CL/*F*, *V*/*F* and k_a were moderate to low with values of 28.6%, 7.7% and 3.0%, respectively. The shrinkage for IOV on CL/*F* was relatively high at 74%, which may be because only approximately 30% patients had sampling on more than one occasion to estimate IOV. The average time of gall bladder emptying (*t*′) was 6.13 h post-dose. The residual proportional error for predicted plasma concentrations was relatively large (51.4%).

Goodness-of-fit plots in Figure 3 show that model predictions were in reasonable agreement with the observed plasma concentrations. The conditional and individual weighted residuals did not reflect any systematic deviations. The predictions at steady-state were much closer to

Table 3

Final PPK model parameter estimates

Parameter	Original data set Typical estimate	2284 Bootstrap replicates* Median	95% CI
CL/*F* ($l\ h^{-1}$)	8.13	7.86	6.98, 10.7
***V*/*F* (l)†**	213	212	196, 232
Mean absorption transit time‡ (h)	1.98	1.98	1.75, 2.25
k_{Ehc} (h^{-1})	0.857	0.81	0.478, 1.26
F_{ent}§	0.498	0.492	0.464, 0.498
***t*′ (h)¶**	6.13	6.32	5.78, 7.34
Proportional residual error (%CV)	51.4	51.4	45.6, 56
Additive residual error ($\times 10^{-3}$) ($mg\ l^{-1}$)	1.0003	1.00002	1.0001, 1.0003
IIV CL/*F* (%CV)	18.0	18.0	1.1, 37
IIV *V*/*F* (%CV)	68.7	72.5	61.2, 79.3
IIV k_a (%CV)	61.9	61.2	55.0, 73.8
IOV CL/*F* (%CV)	47.7	49.4	29.2, 55.2
Correlation $_{CL/F-V/F}$	0.778	0.815	0.181, 0.996

*Results from all 2284 replicates were used to calculate the median and the 95% CI for the PPK model parameters. †Assuming median bodyweight of 80 kg. $F_{ent} = 1/(1 + F_{ents}) = 1/(1 + 0.00542) = 0.498$. ‡Mean absorption transit time = (number of transit compartments+1)/k_a = 5/2.53 = 1.98. §F_{ent} was described as logit function, and actual estimated parameter was F_{ents}. ¶*t*′: absolute time post-dose administration at which EHC starts. IIV, inter-individual variability; IOV, inter-occasion variability.

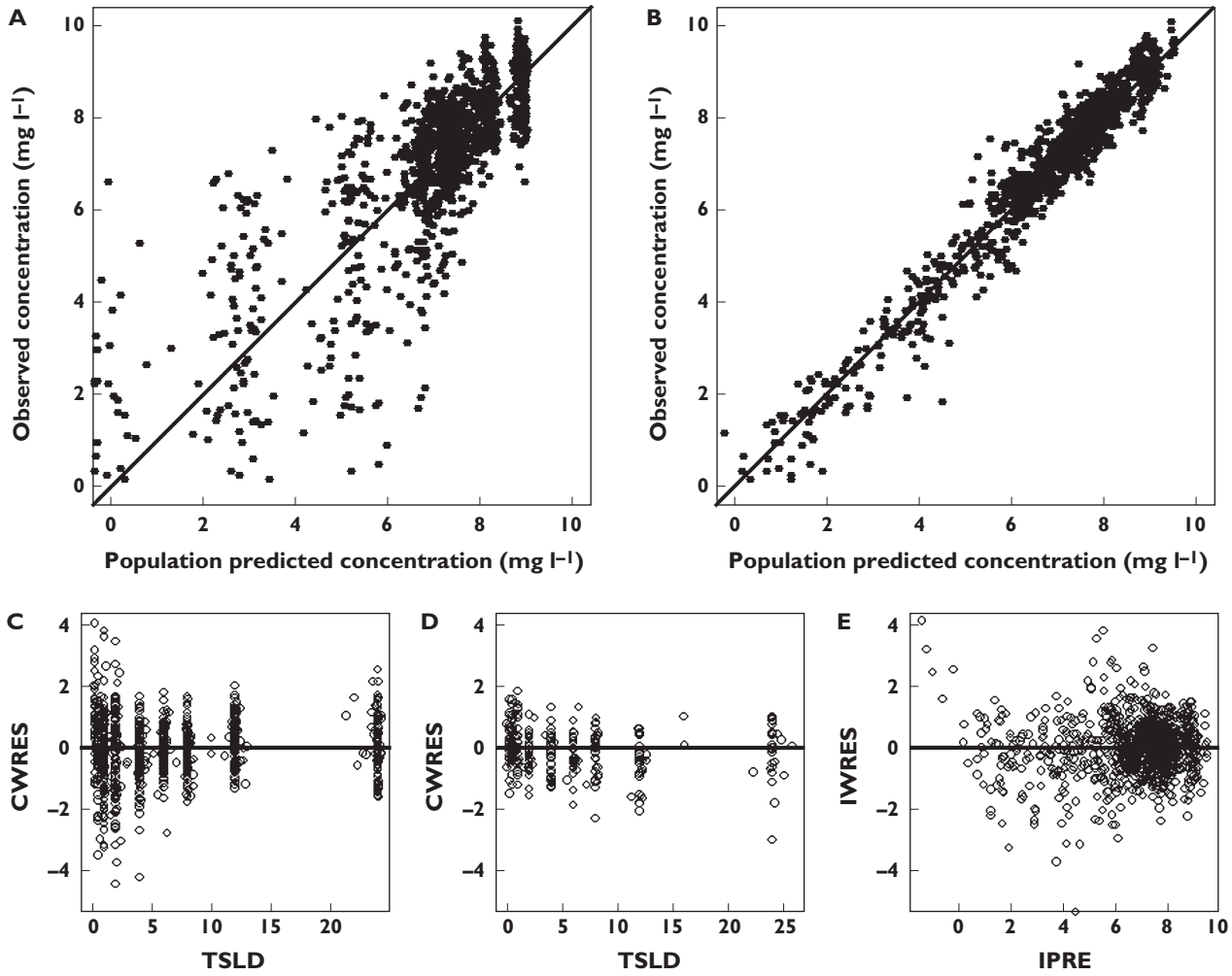

Figure 3

Goodness-of-fit plots for the final PPK model. A) Population-predicted *vs.* observed plasma concentrations on a log-log scale. B) Individual predicted *vs.* observed plasma concentrations on a log-log scale. Conditional weighted residuals (CWRES) *vs.* time since last dose (TSLD, h) (C) after initial doses and (D) at steady-state. E) Individual-weighted residuals (IWRES) *vs.* individual predicted plasma concentrations

the observed concentrations than the predictions after single dose (Figure 3C, D).

Model evaluation

The PPK model evaluation, including the visual predictive checks (VPC), revealed that the final model predictions were in reasonable agreement with observed plasma concentrations. In VPC (Figure 4), dose-normalized measured concentrations were overlaid with the 90% prediction intervals of dose-normalized, model predicted plasma concentrations and observed concentrations, stratified by occasion (i.e. after initial dose and at steady-state). All five summary statistics, 5th percentile, 25th percentile, median, 75th percentile, and 95th percentile, were adequately predicted on both occasions, with no apparent bias. The results suggest that model-simulated exposures from the final PPK model were reasonably close to the observed exposures that were used for PPK model building.

The results of the nonparametric bootstrap analysis are listed in Table 3. Of total 2284 replicates 72.1% converged successfully, indicating that the model was stable. The 95% confidence intervals on structural parameters appeared to be reasonably well estimated but the confidence interval on IIV terms were wider. RE and RMSE were calculated to examine the predictive ability of the model by comparing the model predictions based on typical parameter values with the observed concentrations. The RE and RMSE for each occasion are summarized in Table 4. The range of RE for single dose data was relatively wide, but the 5th, 10th, 85th and 90th percentiles were −12.6%, −1.8%, 5.5% and 20.1%, respectively, suggesting that majority of predictions for single dose had RE of <6%. Predictions for steady-state were closer to the observed data, with RE of < ± 3% for all observations, also evident from Figure 3C, D. The RMSE was calculated using log transformed data and was back transformed in normal scale for summary statistics. The median

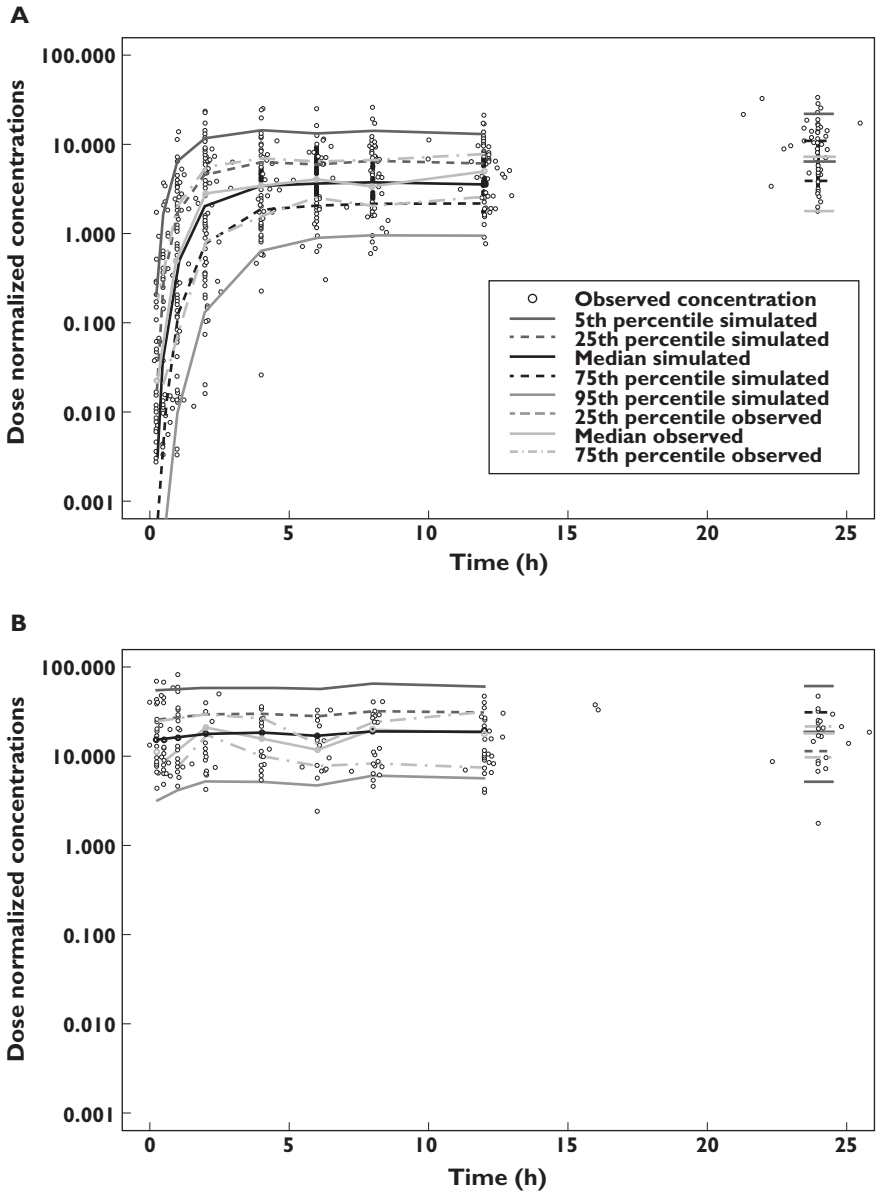

Figure 4

Visual predictive check for final PPK model (A) after initial doses and (B) at steady-state. Solid thick black (▬) and light grey (▬) lines represent the median for simulated and predicted dose normalized concentrations. The solid dim grey lines (▬) show the 5th and 95th percentile and dotted black lines (▪ ▪ ▪) show the 25th and 75th percentile for simulated data. The dotted light grey lines (▪ ▪ ▪) show the 25th and 75th percentile for observed data and dose-normalized observed concentrations are shown as open circles (○)

RMSE values for single dose and steady-state data were <1.5 ng ml^{-1}, suggesting low residual variance with limited bias for predicted concentrations.

Discussion

A semi-mechanistic PPK model was developed and evaluated to describe the oral absorption and systemic PK of sorafenib in patients with solid tumours, using dense plasma concentration–time profiles from two dose levels after initial doses and at steady-state. This is the first model describing sorafenib PK based on its known disposition characteristics such as delayed/solubility-limited GI absorption and EHC, and the estimated PPK parameters were also in agreement with known properties of sorafenib. This model can also be used to simulate and explore alternative dosing regimens and to develop exposure-response relationships. Furthermore, the parameterization of this EHC model is uniquely robust as it does not require a discontinuous function for gall bladder emptying which is characteristic of most such models.

Table 4

Relative error (RE) and root mean square error (RMSE) for predictions from the final model

Parameter	Occasion	Summary statistics Median	5th percentile	95th percentile
RE (%)	Single dose	0.48	–12.6	69.2
	Steady-state	0.35	–0.77	2.0
RMSE* (ng ml^{-1})	Single dose	1.45	1.19	2.41
	Steady-state	1.35	1.16	1.79

*RMSE was calculated for log-transformed data and was back-transformed in normal scale for summary statistics.

The final PK model was a one compartment model with four catenary GI transit absorption compartments and a gall bladder compartment modelling discontinuous EHC. The estimated typical value of CL/*F* (8.13 l h^{-1}) suggests low hepatic extraction of sorafenib, when compared with a hepatic blood flow of 90 l h^{-1}, consistent with predictions based on systemic clearance from preclinical studies [9]. The estimated typical value for apparent volume of distribution (*V*/*F* of 213 l) suggests extensive tissue distribution despite a high degree of plasma protein binding, probably a consequence of sorafenib's high lipophilicity (log P = 3.8) [28]. A previous PPK abstract based on 226 cancer patients and 69 healthy subjects reported lower estimates for CL/*F* and *V*/*F*, respectively, 3.31 l h^{-1} and 110 l [29]. This discrepancy is likely a consequence of the lack of EHC in their model: Since EHC is responsible for 50% of systemic exposure in the current PPK model, the apparent oral bioavailability (*F*) without EHC is reduced by half translating into 2-fold higher CL/*F* and *V*/*F*.

The IIV estimates on CL/*F*, *V*/F and k_a suggested moderate to high variability (%CV 18–68%) between patients, and CL/*F* also randomly varied by occasion (48%). We attempted to separate the IOV on CL and *F* by fixing the *F* to 1, but the model did not support this parameterization with available data. Based on the known disposition profile of sorafenib, its CL and/or *F* may randomly change between occasions because of differences in solubility, food–drug interaction, and possible alteration in activity of metabolic enzymes and transporters.

Consistent with the findings of a clinical study reporting no significant effect of ketoconazole co-administration on sorafenib exposures [30], genetic variations in CYP enzymes (CYP3A4*1B and CYP3A5*3C) were not related to sorafenib PK. The glucuronidation pathway was reported to be more important than the oxidation pathway for sorafenib metabolism [30]. A single patient carrying the UGT1A9*3*3 genotype appeared to have approximately 2-fold lower CL/*F* and *V*/*F* values than carriers of either the UGT1A9*1*1 (n = 103) or UGT1A9*1*3 (n = 3) genotype. However, this effect could not be evaluated statistically because of the small sample size. Inspection of individual objective function values and a leverage analysis on a subset of data from patients who had non-*3 alleles suggested that UGT1A9*3 genotype is likely not important for estimation of PK parameters.

A prospective clinical PK study evaluating the impact of chronic hepatic and renal dysfunction on single dose sorafenib PK, failed to find any association between organ function and systemic sorafenib exposure, even by enrolling patients with severe liver and kidney impairment (n = 138) [31]. As the patients enrolled on our clinical trials were required to have adequate organ function, it was less likely for these covariates to have shown any significant effects in our analysis. Of the other covariates evaluated, bodyweight was significant for *V*/*F* in our patients, but its contribution was rather small (4% decrease in IIV), and a large portion of variability in *V*/*F* (68%) remained unaccounted for in the final PPK model.

We observed that the GI transit compartments model adequately described the lag time in the early plasma concentration–time profiles and stabilized the model and estimation of k_a as compared with other investigated models. Use of a single first order process (k_a) to describe the GI absorption is limited due to the multiple processes and mechanisms involved in GI absorption [32]. Description of initial delay in the appearance of quantifiable plasma concentrations by a simple lag time assumes a sudden increase in GI drug absorption during GI transit, which is physiologically unrealistic, and may also cause numerical instability during integration of differential model equations [33]. In contrast, the GI transit compartment model describes the absorption phase as a gradually changing, continuous function, which seems to reflect better the physiologic absorption process [33].

A common feature of EHC models is the use of a variable number of caternary compartments between the central (systemic circulation) and absorption compartments (GI tract). Generally, a fraction of drug in the systemic circulation is excreted into the bile compartment, which is then re-circulated into the GI absorption transit compartment at a zero order rate or at periodic intervals (such as regulated by sine wave function) or at *a priori* known times (e.g. times of food intake) [24, 34]. We evaluated several of these EHC models and found that the EHC model with emptying at regular intervals was most suitable for our dataset.

The final PPK model evaluation was performed with VPC, bootstrap analysis, and estimation of RE and RMSE. The VPC graphically compares aggregate observed plasma concentration–time data and 90% prediction intervals derived from model-simulated data. A non-parametric bootstrap analysis was performed to evaluate the precision of estimated PK parameters. 72.1% of the bootstrap replicates converged successfully. The bootstrap showed narrow confidence intervals for all parameters. The estimation of RMSE and RE demonstrated low residual variance and little bias for predictions and relatively low prediction errors for steady-state concentrations compared with concentrations after single dose.

In summary, this study presents a semi-mechanistic PPK model of oral sorafenib in patients with various solid tumours. Although we successfully developed a PPK model that accounted for delayed absorption and EHC, the residual error for plasma concentrations remained high (approximately 50%). This could have been a consequence of the heterogeneity among the studied patient population [35] as well as model mis-specification. While the model attempted to account for sorafenib's known biopharmaceutical properties to describe the available data, given the characteristics of sorafenib (e.g. low solubility and complex disposition) the high residual error is not unexpected. Apparently, the previous PPK model for sorafenib also reported a high residual error of 48% [29]. Furthermore, cancer patients are inherently heterogeneous due to their disease and the effects of prior and current treatments, which can alter hepatic and other physiological functioning. Genetic variation in CYP3A4 and CYP3A5 did not appear to alter sorafenib disposition. The UGT1A9*3 polymorphism also does not appear to be an important determinant for sorafenib pharmacokinetics.

Competing Interests

Sorafenib was supplied to the National Cancer Institute (NCI) from Bayer Health Corp under a CRADA negotiated with the Cancer Therapy Evaluation Program (CTEP). CTEP in turn supplied the sorafenib for this study. RY is a co-inventor on one or more US and/or foreign patents (or outstanding patent applications) involving interleukin-12 as a treamtnet for Kaposi's sarcoma. All rights, title, and interest to these patents have been or should by law be assigned to the U.S. Department of Health and Human Services. The government conveys a portion of the royalties it receives to its employee inventors under the Federal Technology Transfer Act of 1986 (P.L. 99–502). There are no other competing interests to declare.

Disclaimer

The content of this publication does not necessarily reflect the views or policies of the Department of Health and Human Services, nor does mention of trade names, commercial products, or organizations imply endorsement by the U.S. Government.

This project has been funded in whole or in part with federal funds from the National Cancer Institute, National Institutes of Health, under contract HHSN261200800001E (ERG). This work was supported by the Intramural Research Program of the NIH, National Cancer Institute, Center for Cancer Research.

We thank our research nurses and data managers Ms Cynthia Graves, Ms Sonja Crandon, Mr Qinghua Ge (Roger), Ms Shveta Tiwari and Ms Kathleen Wyvill, and most of all, our patients who participated in these trials.

REFERENCES

1 Onyx Pharmaceuticals. Nexavar (Sorafenib) tablets. Available at http://www.onyx-pharm.com/view.cfm/3/Products-Overview (last accessed 8 July 2010).

2 Wilhelm S, Carter C, Lynch M, Lowinger T, Dumas J, Smith RA, Schwartz B, Simantov R, Kelley S. Discovery and development of sorafenib: a multikinase inhibitor for treating cancer. Nat Rev Drug Discov 2006; 5: 835–44.

3 Bayer Pharmaceuticals. Nexavar (Sorafenib) Prescribing Information. Available at http://www.nexavar.com/html/download/Nexavar_PI.pdf (last accessed 8 July 2010).

4 Awada A, Hendlisz A, Gil T, Bartholomeus S, Mano M, de Valeriola D, Strumberg D, Brendel E, Haase CG, Schwartz B, Piccart M. Phase I safety and pharmacokinetics of BAY 43-9006 administered for 21 days on/7 days off in patients with advanced, refractory solid tumours. Br J Cancer 2005; 92: 1855–61.

5 Clark JW, Eder JP, Ryan D, Lathia C, Lenz HJ. Safety and pharmacokinetics of the dual action Raf kinase and vascular endothelial growth factor receptor inhibitor, BAY 43-9006, in patients with advanced, refractory solid tumors. Clin Cancer Res 2005; 11: 5472–80.

6 Moore M, Hirte HW, Siu L, Oza A, Hotte SJ, Petrenciuc O, Cihon F, Lathia C, Schwartz B. Phase I study to determine the safety and pharmacokinetics of the novel Raf kinase and VEGFR inhibitor BAY 43-9006, administered for 28 days on/7 days off in patients with advanced, refractory solid tumors. Ann Oncol 2005; 16: 1688–94.

7 Strumberg D, Clark JW, Awada A, Moore MJ, Richly H, Hendlisz A, Hirte HW, Eder JP, Lenz HJ, Schwartz B. Safety, pharmacokinetics, and preliminary antitumor activity of sorafenib: a review of four phase I trials in patients with advanced refractory solid tumors. Oncologist 2007; 12: 426–37.

8 Strumberg D, Richly H, Hilger RA, Schleucher N, Korfee S, Tewes M, Faghih M, Brendel E, Voliotis D, Haase CG, Schwartz B, Awada A, Voigtmann R, Scheulen ME, Seeber S. Phase I clinical and pharmacokinetic study of the novel Raf kinase and vascular endothelial growth factor receptor inhibitor BAY 43-9006 in patients with advanced refractory solid tumors. J Clin Oncol 2005; 23: 965–72.

9 Nexavar: European Public Assessment Reports (EPAR)-Scientific Discussion. European Medicines Agency (EMA). Available at http://www.ema.europa.eu/docs/en_GB/document_library/EPAR_-_Scientific_Discussion/human/000690/WC500027707.pdf (last accessed 1 April 2011).

10 Amidon GL, Lennernas H, Shah VP, Crison JR. A theoretical basis for a biopharmaceutic drug classification: the correlation of *in vitro* drug product dissolution and *in vivo* bioavailability. Pharm Res 1995; 12: 413–20.

11 He P, Court MH, Greenblatt DJ, Von Moltke LL. Genotype-phenotype associations of cytochrome P450 3A4

and 3A5 polymorphism with midazolam clearance *in vivo*. Clin Pharmacol Ther 2005; 77: 373–87.

12 Bosch TM, Meijerman I, Beijnen JH, Schellens JH. Genetic polymorphisms of drug-metabolising enzymes and drug transporters in the chemotherapeutic treatment of cancer. Clin Pharmacokinet 2006; 45: 253–85.

13 Domanski TL, Finta C, Halpert JR, Zaphiropoulos PG. cDNA cloning and initial characterization of CYP3A43, a novel human cytochrome P450. Mol Pharmacol 2001; 59: 386–92.

14 Gomo C, Coriat R, Faivre L, Mir O, Ropert S, Billemont B, Dauphin A, Tod M, Goldwasser F, Blanchet B. Pharmacokinetic interaction involving sorafenib and the calcium-channel blocker felodipine in a patient with hepatocellular carcinoma. Invest New Drugs 2010. DOI: 10.1007/s10637-010-9514-3.

15 Girard H, Court MH, Bernard O, Fortier LC, Villeneuve L, Hao Q, Greenblatt DJ, von Moltke LL, Perussed L, Guillemette C. Identification of common polymorphisms in the promoter of the UGT1A9 gene: evidence that UGT1A9 protein and activity levels are strongly genetically controlled in the liver. Pharmacogenetics 2004; 14: 501–15.

16 Mross K, Steinbild S, Baas F, Gmehling D, Radtke M, Voliotis D, Brendel E, Christensen O, Unger C. Results from an *in vitro* and a clinical/pharmacological phase I study with the combination irinotecan and sorafenib. Eur J Cancer 2007; 13: 55–63.

17 Villeneuve L, Girard H, Fortier LC, Gagne JF, Guillemette C. Novel functional polymorphisms in the UGT1A7 and UGT1A9 glucuronidating enzymes in Caucasian and African-American subjects and their impact on the metabolism of 7-ethyl-10-hydroxycamptothecin and flavopiridol anticancer drugs. J Pharmacol Exp Ther 2003; 307: 117–28.

18 Paoluzzi L, Singh AS, Price DK, Danesi R, Mathijssen RH, Verweij J, Figg WD, Sparreboom A. Influence of genetic variants in UGT1A1 and UGT1A9 on the *in vivo* glucuronidation of SN-38. J Clin Pharmacol 2004; 44: 854–60.

19 Lepper ER, Baker SD, Permenter M, Ries N, van Schaik RH, Schenk PW, Price DK, Ahn D, Smith NF, Cusatis G, Ingersoll RG, Bates SE, Mathijssen RH, Verweij J, Figg WD, Sparreboom A. Effect of common CYP3A4 and CYP3A5 variants on the pharmacokinetics of the cytochrome P450 3A phenotyping probe midazolam in cancer patients. Clin Cancer Res 2005; 11: 7398–404.

20 Jain L, Gardner ER, Venitz J, Dahut W, Figg WD. Development of a rapid and sensitive LC-MS/MS assay for the determination of sorafenib in human plasma. J Pharm Biomed Anal 2008; 46: 362–7.

21 Bonate PL, Floret S, Bentzen C. Population pharmacokinetics of APOMINE: a meta-analysis in cancer patients and healthy males. Br J Clin Pharmacol 2004; 58: 142–55.

22 NMusers (NONMEM UsersNet Archive). Adaptation of multiple-dose enterohepatic circulation model suggested by Luann Phillips (after Stuart Beal). (11 June 2002).

23 Jiao Z, Ding JJ, Shen J, Liang HQ, Zhong LJ, Wang Y, Zhong MK, Lu WY. Population pharmacokinetic modelling for enterohepatic circulation of mycophenolic acid in healthy Chinese and the influence of polymorphisms in UGT1A9. Br J Clin Pharmacol 2008; 65: 893–907.

24 Moon YJ, Wang L, DiCenzo R, Morris ME. Quercetin pharmacokinetics in humans. Biopharm Drug Dispos 2008; 29: 205–17.

25 Mould DR, Sweeney K, Duffull SB, Neylon E, Hamlin P, Horwitz S, Sirotnak F, Fleisher M, Saunders ME, O'Connor OA. A population pharmacokinetic and pharmacodynamic evaluation of pralatrexate in patients with relapsed or refractory non-Hodgkin's or Hodgkin's lymphoma. Clin Pharmacol Ther 2009; 86: 190–6.

26 Savic RM, Karlsson MO. Importance of shrinkage in empirical bayes estimates for diagnostics: problems and solutions. AAPS J 2009; 11: 558–69.

27 West GB, Brown JH, Enquist BJ. A general model for the origin of allometric scaling laws in biology. Science 1997; 276: 122–6.

28 Drug Bank. Sorafenib drug card DB00398. Available at http://www.drugbank.ca/search/search?query=sorafenib (last accessed 8 July 2010).

29 Rajagopalan P, Lathia C, Sundaresan P. Population Pharmacokinetics of Sorafenib in Cancer Patients. San Diego, CA: American Association of Pharmaceutical Sciences (AAPS), 2007.

30 Lathia C, Lettieri J, Cihon F, Gallentine M, Radtke M, Sundaresan P. Lack of effect of ketoconazole-mediated CYP3A inhibition on sorafenib clinical pharmacokinetics. Cancer Chemother Pharmacol 2006; 57: 685–92.

31 Miller AA, Murry DJ, Owzar K, Hollis DR, Kennedy EB, Abou-Alfa G, Desai A, Hwang J, Villalona-Calero MA, Dees EC, Lewis LD, Fakih MG, Edelman MJ, Millard F, Frank RC, Hohl RJ, Ratain MJ. Phase I and pharmacokinetic study of sorafenib in patients with hepatic or renal dysfunction: CALGB 60301. J Clin Oncol 2009; 27: 1800–5.

32 Bonate PL. Pharmacokinetic-Pharmacodynamic Modeling and Simulation, 1st edn. New York: Springer, 2006; 248–9.

33 Savic RM, Jonker DM, Kerbusch T, Karlsson MO. Implementation of a transit compartment model for describing drug absorption in pharmacokinetic studies. J Pharmacokinet Pharmacodyn 2007; 34: 711–26.

34 Ette EI, Williams PJ, eds. Pharmacometrics: The Science of Quantitative Pharmacology. New Jersey: Wiley, John & Sons, Incorporated, 2007; 351–59.

35 Karlsson MO, Beal SL, Sheiner LB. Three new residual error models for population PK/PD analyses. J Pharmacokinet Biopharm 1995; 23: 651–72.

Supporting Information

Additional Supporting Information may be found in the online version of this article:

Table S1
Comparison of PK parameters for models with and without weight as covariate

Please note: Wiley-Blackwell are not responsible for the content or functionality of any supporting materials supplied by the authors. Any queries (other than missing material) should be directed to the corresponding author for the article.